J Mater Sci (2009) 44:5515–5523
DOI 10.1007/s10853-009-3771-6

Magnetoelectric and electrical properties of WO_3-doped $(Ni_{0.8}Zn_{0.1}Cu_{0.1})Fe_2O_4$/[$Pb(Ni_{1/3}Nb_{2/3})O_3$–$Pb(Zn_{1/3}Nb_{2/3})O_3$–$PbTiO_3$] composites

Renbing Sun · Bijun Fang · Xinwei Dong · Junming Liu

Received: 13 January 2009 / Accepted: 21 July 2009 / Published online: 4 August 2009

Abstract A total of 5 mol% WO_3-doped $(1-x)(Ni_{0.8}Zn_{0.1}Cu_{0.1})Fe_2O_4/xPb(Ni_{1/3}Nb_{2/3})O_3$–$Pb(Zn_{1/3}Nb_{2/3})O_3$–$PbTiO_3$ ($(1-x)$NZCF/xPNN-PZN-PT) magnetoelectric particulate ceramic composites were prepared by conventional solid-state reaction method via low-temperature sintering process. X-ray diffraction (XRD) measurement and scanning electron microscopy (SEM) observation indicate that piezoelectric phase and ferrite phase coexist in the sintered particulate ceramic composites. Dielectric property of the $(1-x)$NZCF/x0.53PNN–0.02PZN–0.05$Pb(Ni_{1/2}W_{1/2})O_3$–0.40PT ($(1-x)$NZCF/xPNN-PZN-PNW-PT, nominal composition) composites is improved greatly as compared to that of the undoped $(1-x)$NZCF/xPNN-PZN-PT composites. The WO_3-doped $(1-x)$NZCF/xPNN-PZN-PT composites exhibit typical P–E hysteresis loops at room temperature accompanied by the decrease of saturation polarization (P_s) and remnant polarization (P_r). At the same time, piezoelectric property of the composites deteriorates greatly with the increase of ferrite content. The $(1-x)$NZCF/xPNN-PZN-PNW-PT composites can be electrically and magnetically poled and exhibit apparent magnetoelectric (ME) effect. A maximum ME voltage coefficient of 13.1 mV/(cm Oe) is obtained in the 0.1NZCF/0.9PNN-PZN-PNW-PT composite at 400 Oe d.c. magnetic bias field superimposed 1 kHz a.c. magnetic field with 5 Oe amplitude. The addition of WO_3 in the piezoelectric phase decreases sintering temperature greatly from 1180 °C to 950 °C and decreases dielectric loss sharply of the composites, thus the ME voltage coefficient increases. Such ceramic processing is valuable for the preparation of magnetoelectric particulate ceramic composites with excellent ME effect.

R. Sun · B. Fang (✉)
School of Materials Science and Engineering, Jiangsu Polytechnic University, Changzhou, Jiangsu 213164, People's Republic of China
e-mail: fangbj@em.jpu.edu.cn

R. Sun · B. Fang
Key Laboratory for Polymer Materials, Changzhou, Jiangsu 213164, People's Republic of China

X. Dong · J. Liu
National Laboratory of Solid State Microstructures, Nanjing University, Nanjing, Jiangsu 210093, People's Republic of China

Introduction

Recently, extensive research has been concentrated on the magnetoelectric materials due to their potential device applications. The magnetoelectric effect (ME) is defined as a variation of dielectric polarization in the system as a response to an applied magnetic field $(ME)_H$ or an induced magnetization by an external electric field $(ME)_E$ [1, 2]. The ME effect shows the possibility of effective conversion between electric energy and magnetic energy, which provides opportunity for potential applications in ME memories, waveguides, transducers, actuators, sensors, and heterogeneous read/write devices [3, 4].

The ME effect can be dated back to as early as 1894, when Curie pointed out that it would be possible for an asymmetric molecular body to polarize directionally under the influence of a magnetic field. Later, Landau and Lifshitz showed that in terms of crystal symmetry a linear ME effect could occur in a magnetically ordered crystals. Subsequently, Dzyaloshinskii, on the basis of theoretical analysis, predicted the existence of the ME effect in antiferromagnetic Cr_2O_3. This was confirmed by Astrov who measured the magnetization induced by electric field and

later by Rado and Folen who detected the polarization induced by magnetic field. Then a lot of single-phase materials exhibiting ME effect have been discovered in the last few decades [5–7]. However, due to a poor ME output and a very low Neel or Curie temperature, it was not successful to use single-phase materials in ME device applications.

In contrast, two-phase magnetoelectric composites composed of piezoelectric and magnetic materials have drawn significant interest in recent years, in which the coupling interaction between the piezoelectric and magnetic materials could produce a large ME response [8–22]. The ME effect in composites is a result of a product tensor property, which was proposed by Van Suchetelene in 1972 [2]. That is, for the $(ME)_H$ effect, when a magnetic field is applied to the two-phase composite, the magnetostrictive phase changes its shape firstly, and the induced stress is passed to the piezoelectric phase, generating an electric polarization proportional to the applied magnetic field. Therefore, the ME effect in composites is extrinsic response, which depends on the composite microstructure and the coupling interaction across the magnetic-piezoelectric interfaces [20, 22].

So far, three kinds of bulk magnetoelectric composites have been investigated in experimental and theoretical, i.e., composites of (a) ferrite and piezoelectric ceramics, (b) magnetic metals/alloys and piezoelectric ceramics, and (c) Terfenol-D embedded in piezoelectric polymer or ceramic matrix. In terms of phase connectivity, 0-3, 3-3, 2-2, and 1-3 type structured multiferroic composites have been developed in a two-phase composite. The elastic coupling interaction between the magnetostrictive phase and piezoelectric phase leads to giant ME response of these magnetoelectric composites. The maximum ME coefficient in the 2-2 type laminate composites reaches the order of V/(cm Oe) [20, 21], which exceeds the ME response of single-phase compounds by many orders of magnitude. As compared to laminated composites, sintered particulate composites exhibit inferior ME property due to the drawbacks such as low resistivity, interface defects, interface diffusion, mismatch in elastic compliance, and degradation in individual material parameters. Therefore, in spite of the high theoretical ME coefficients of the particulate composite ceramics, it is difficult to achieve the predicted values in experimental [20–22].

It is known that low anisotropy favors the magnetization mechanism in crystal, such as domain wall movement and domain rotation, which are the key factors for magneto-mechanical coupling that give rise to the ME effect. Hence, soft ferrite $NiFe_2O_4$ with low anisotropy and high initial permeability is a promising candidate. Furthermore, a larger net magnetic moment caused by the ion rearrangement, which favors the ME effect, can be obtained by substituting some zinc into nickel ferrite. On the other hand, $Pb(Ni_{1/3}Nb_{2/3})O_3$-$PbTiO_3$ and $Pb(Zn_{1/3}Nb_{2/3})O_3$ are also known to exhibit large piezoelectric response. The addition of WO_3 in the ferroelectric phase can improve the densification of the ceramic composites and greatly decrease the sintering temperature [23, 24], thus improving the ME effect. The addition of CuO can also decrease sintering temperature and reduce the interdiffusion between the piezoelectric and ferrite phases.

In this paper, particulate ceramic composites composed of ferrite $(Ni_{0.8}Zn_{0.1}Cu_{0.1})Fe_2O_4$ (NZCF) and relaxor-based ferroelectric $(1-x-y)Pb(Ni_{1/3}Nb_{2/3})O_3$–$xPb(Zn_{1/3}Nb_{2/3})O_3$–$yPbTiO_3$ (PNN-PZN-PT) end members were prepared by conventional solid-state reaction method. Particulate composites were investigated due to the advantageous of cost effectiveness, easy fabrication process, and better control of process parameters. To inhibit the interdiffusion between piezoelectric and ferrite phases and improve the ME effect of the particulate composites, WO_3 and CuO were used as sintering aids to decrease sintering temperature and to increase relative density. The magnetoelectric, dielectric, piezoelectric, and ferroelectric properties of the WO_3-doped $(1-x)$NZCF/xPNN-PZN-PT composites were studied systematically accompanied by the observation of microstructure and the analysis of chemical composition and elemental diffusion in order to clarify the possible mechanism of the ME effect.

Experimental procedure

Magnetoelectric particulate ceramic composites consist of piezoelectric phase and ferrite phase were prepared by conventional solid-state reaction method. Analytical-purity oxides, NiO, ZnO, CuO, Fe_2O_3, PbO, Nb_2O_5, WO_3, and TiO_2, were used as raw materials. For the preparation of $(Ni_{0.8}Zn_{0.1}Cu_{0.1})Fe_2O_4$ (NZCF) ferrite, stoichiometric mixture of raw oxides was ball-milled in distilled water for 12 h, then the mixed slurry was dried and calcined at 1000 °C for 3 h in air. For the preparation of $0.58Pb(Ni_{1/3}Nb_{2/3})O_3$-$0.02\ Pb(Zn_{1/3}Nb_{2/3})O_3$-$0.40PbTiO_3$ (0.58PNN-0.02 PZN-0.40PT) ferroelectric, the columbite precursor method was adopted. In the first stage, the columbite precursors, $NiNb_2O_6$ and $ZnNb_2O_6$, were synthesized by calcining of a mixture of stoichiometric NiO and ZnO with Nb_2O_5, respectively, at 1000 °C for 4 h. In the second stage, stoichiometric PbO and TiO_2 were added to the above precursors and the mixture was also wet ball-milling using ZrO_2 milling media, then the mixture was dried and calcined at 900 °C for 2 h in air.

Particulate magnetoelectric ceramic composites were prepared by conventional ceramic processing using the above synthesized ferrite and piezoelectric precursors

according to the formula $(1-x)$NZCF/xPNN-PZN-PT (x = 1.0, 0.9, 0.8, and 0.7, weight ratio). The stoichiometric mixed powders were uniaxially pressed into cylindrical pellets with 12 mm in diameter and 2 mm in thickness with the addition of about 3 wt% polyvinyl alcohol (PVA, the concentration of the PVA water solution is 8 wt%) binder and sintered at 1180 °C for 2 h in air and then furnace cooled. To improve dielectric and magnetoelectric properties of the particulate ceramic composites, 5 mol% WO_3 was added to the $(1-x)$NZCF/xPNN-PZN-PT system (designed as nominal composition $(1-x)$NZCF/x0.53PNN–0.02PZN-0.05Pb($Ni_{1/2}W_{1/2}$)O_3–0.40PT, abbreviated as $(1-x)$NZCF/xPNN-PZN-PNW-PT) as sintering aid, which decreases the sintering temperature of the composites as being 950 °C for 2 h. Such amount of WO_3 doping and sintering conditions are sufficient to obtain particulate ceramic composites with high densification [24].

Crystal structure of the sintered particulate ceramic composites was characterized by the X-ray powder diffraction measurement (XRD, D/max-2500/PC Rigaku X-ray Diffractionmeter) using Cu Kα radiation. Microstructure of the samples was observed by scanning electron microscopy (SEM, Hitachi S-4800 Field Emissiom Scanning Electron Microscope) using free surfaces of the specimens after thermal etching at 825 °C for 30 min. X-ray elemental analysis was performed by a INCA energy dispersive X-ray analysis (EDX) attached to the SEM equipment in order to identify any elemental interdiffusion through the interfaces. For magnetoelectric and electrical properties measurement, silver paste was fired on both surfaces of the well-polished pellets as electrodes. Dielectric property was measured by a computer-interfaced LCR impedance analyzer, under a weak oscillation level of 1.0 V_{rms} (HP4284A). Dielectric hysteresis loops were measured by a Radiant P-LC100 Ferroelectric Test System. The specimens were immersed in silicon oil to prevent arcing. Piezoelectric property was measured by a ZJ-3AN Berlincourt-type quasistatic d_{33} meter after the specimens were electrically poled along the thickness direction. The electrical poling was conducted by applying a electric field of 2 kV/mm at 120–125 °C for 30 min in silicon oil and then slowly cooled down to room temperature in the presence of half of the applied electrical field. For the ME effect measurement, an electromagnet, equipped with water-cooled solenoids, was used, which could generate a d.c. magnetic bias H_{bias} up to 3 kOe. A pair of Helmholtz coils were used to produce an a.c. magnetic field H_{ac} of 5 Oe, which was superimposed on H_{bias}. Prior to the ME measurement, the samples were electrically and magnetically poled along the thickness direction. The electrical poling has been conducted for the measurement of piezoelectric property. The magnetical poling was performed along the same direction as that of the electrical poling by a d.c. magnetic field of 3 kOe for 30 min at room temperature.

Results and discussion

Phase identification and microstructure

XRD patterns of the sintered ferroelectric, ferrite, and particulate ceramic composites are shown in Fig. 1 using $(1-x)$NZCF/xPNN-PZN-PNW-PT as examples. All the diffraction peaks of the piezoelectric phase and ferrite phase are identified in the end members, respectively. The characteristic 2θ values of the diffraction peaks correspond well with the literature reports and the XRD patterns are indexed based on the JCPDS data of ferroelectric Pb($Ni_{1/3}Nb_{2/3}$)O_3 and spinel ferrite $NiFe_2O_4$ (JCPDS files 34-0103 and 74-2081). In the particulate ceramic composites, the diffraction peaks corresponding to PNN-PZN-PNW-PT and NZCF are identified from their individual XRD patterns, indicating the coexistence of piezoelectric and ferrite phases. A systematic variation of the diffraction intensities of the piezoelectric and ferrite phases is observed, which correlates with the variation of the content of the participating phases in the composites. All the peaks can be identified corresponding to their parent phases except for slight content of $Pb_3Nb_4O_{13}$-type pyrochlore phase (marked by *), indicating that no apparent chemical reaction takes place and no intermediate phases form in the synthesized composites. Therefore, particulate ceramic composites composed of piezoelectric and ferrite phases form after sintering and the synthesized composites can be viewed as 3-0 or 0-3 composite system. The formation of slight content of pyrochlore phase can be attributed to the

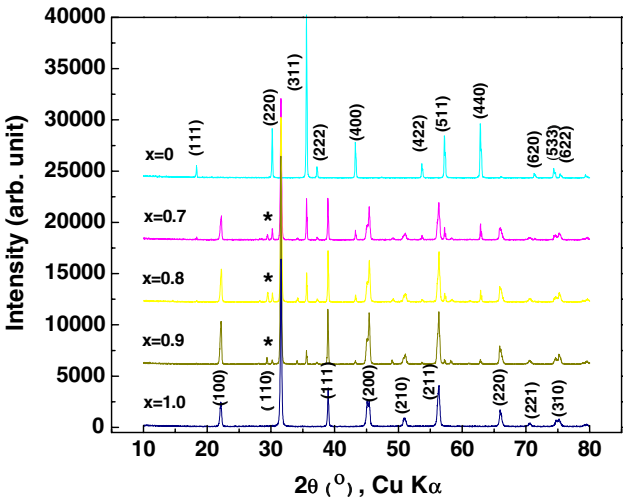

Fig. 1 XRD patterns of the $(1-x)$NZCF/xPNN-PZN-PNW-PT particulate ceramic composite system sintered at 950 °C for 2 h

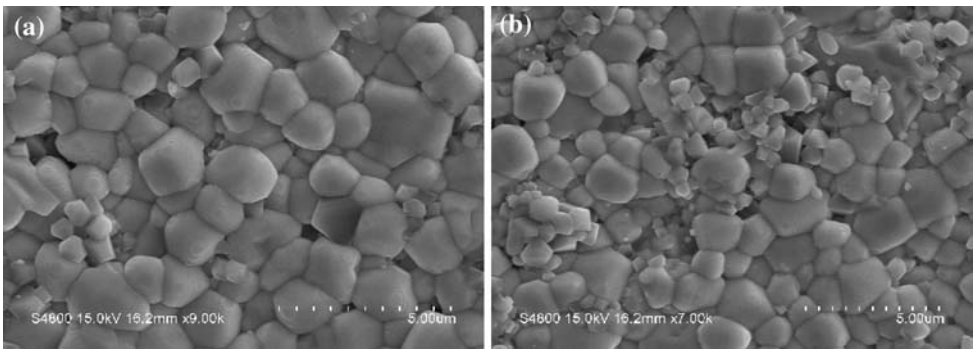

Fig. 2 Secondary electron images of free surface of the $(1-x)$NZCF/xPNN-PZN-PNW-PT particulate ceramic composites sintered at 950 °C for 2 h after thermal etching at 825 °C for 30 min **a** $x = 0.9$ **b** $x = 0.8$

deficiency of Pb^{2+} in the piezoelectric phase near grain boundaries due to the interfacial diffusion of Pb^{2+} into the ferrite [24], which can be confirmed by EDX analysis.

Figure 2 shows the secondary electron images of the $(1-x)$NZCF/xPNN-PZN-PNW-PT particulate ceramic composites with $x = 0.9$ and $x = 0.8$. The sintered composites exhibit rather homogenous micro-morphology, where small granules disperse almost uniformly in large granules. Since physical properties of multiphase composites depend critically on microstructure, it is desirable to know the distribution of the constituent phases. Two distinct phases, the piezoelectric phase with large grains and the ferrite phase with small grains, are clearly seen in the composites. Such consideration is confirmed by EDX analysis as shown in Fig. 3 and Table 1. In the large grains, the contents of Pb and Nb elements are the largest, indicating that the matrix is piezoelectric phase. As a comparison, Ni and Fe elements are the most in the small grains, indicating the existence of ferrite phase. However, Fe element existing in the large grains and Pb element appearing in the small grains prove the existence of ion diffusion between grain boundaries. The absence of W and Zn excitation energy peaks in the ferroelectric grains maybe attributed to the energy limitation of EDX analysis or to the masking of the characteristic excitation peaks of these elements by other ions. However, due to the sight difference of ionic radius (ionic radius of W^{6+}, Ni^{2+}, Zn^{2+}, Ti^{4+}, and Nb^{5+} is 0.60, 0.69, 0.740, 0.605, and 0.64Å, respectively) and the distortion of the phase-pure perovskite cell lattice, W^{6+} tends to replace the above elements and occupies B-site of the perovskite structure.

Dielectric property of the composites

In the sintered particulate ceramic composites, the average grain size of the piezoelectric phase is larger than that of the ferrite phase, which plays crucial role not only in the combined properties (dielectric constant, resistivity, etc.) but also in the product properties such as the ME effect. Frequency and temperature dependence of dielectric property of the $(1-x)$NZCF/xPNN-PZN-PT ($x = 1.0$, $x = 0.9$, $x = 0.8$, $x = 0.7$, weight ratio) composites sintered at 1180 °C for 2 h are shown in Fig. 4. At room temperature, with the increase of the content of NZCF ferrite phase, dielectric constant and loss tangent of the composites increase greatly accompanied by strong frequency dispersion at low frequencies. As a comparison, pure PNN-PZN-PT ceramics exhibit less dielectric frequency dispersion and a broad dielectric response peak appears at around 138 °C. With the increase of NZCF content, the temperature of dielectric maximum (T_m) increases greatly and the dielectric peak becomes blurry gradually accompanied by astonishing increase of the value of dielectric constant. Dielectric loss of all the composites is greatly larger than that of the pure PNN-PZN-PT. The abnormal increase of dielectric constant of the $(1-x)$NZCF/xPNN-PZN-PT composites can be attributed to the high electrical conductivity of ferrite and the charge accumulation on the interfaces of heterogeneous conduction grains induced by ion interdiffusion between piezoelectric and ferrite phases [25]. Strong dielectric frequency dispersion is observed in the magnetoelectric particulate ceramic composites, which can be attributed two possible mechanisms. The first question correlates with the occupation positions of Ni^{2+}, Zn^{2+}, and Nb^{5+} in the $PbTiO_3$ host lattice. Although the substituted ions are "self compensating", i.e., their average charge is equal to the charge of the host Ti^{4+} ion, they distribute randomly and heterogeneously in the $PbTiO_3$ matrix. Therefore, the heterovalent ions need additional local charge compensation, which may be proceeded through the formation of either free charge carriers or the host ion vacancies [26]. These means of local charge compensation lead to the dielectric relaxation of PNN-PZN-PT ferroelectric especially with low content of $PbTiO_3$ in the solid solution. The second possible mechanism is the Maxwell-Wagner relaxation mechanism [27]. Due to the semi-conductivity of ferrite and the interdiffusion of Fe^{3+} and Pb^{2+} between the interfaces of piezoelectric and ferrite phases, different conductive and charge-carrier mobile properties of grains and grain boundaries are engendered. Furthermore, space charges accumulate in the interfaces. Therefore, the strong dielectric frequency

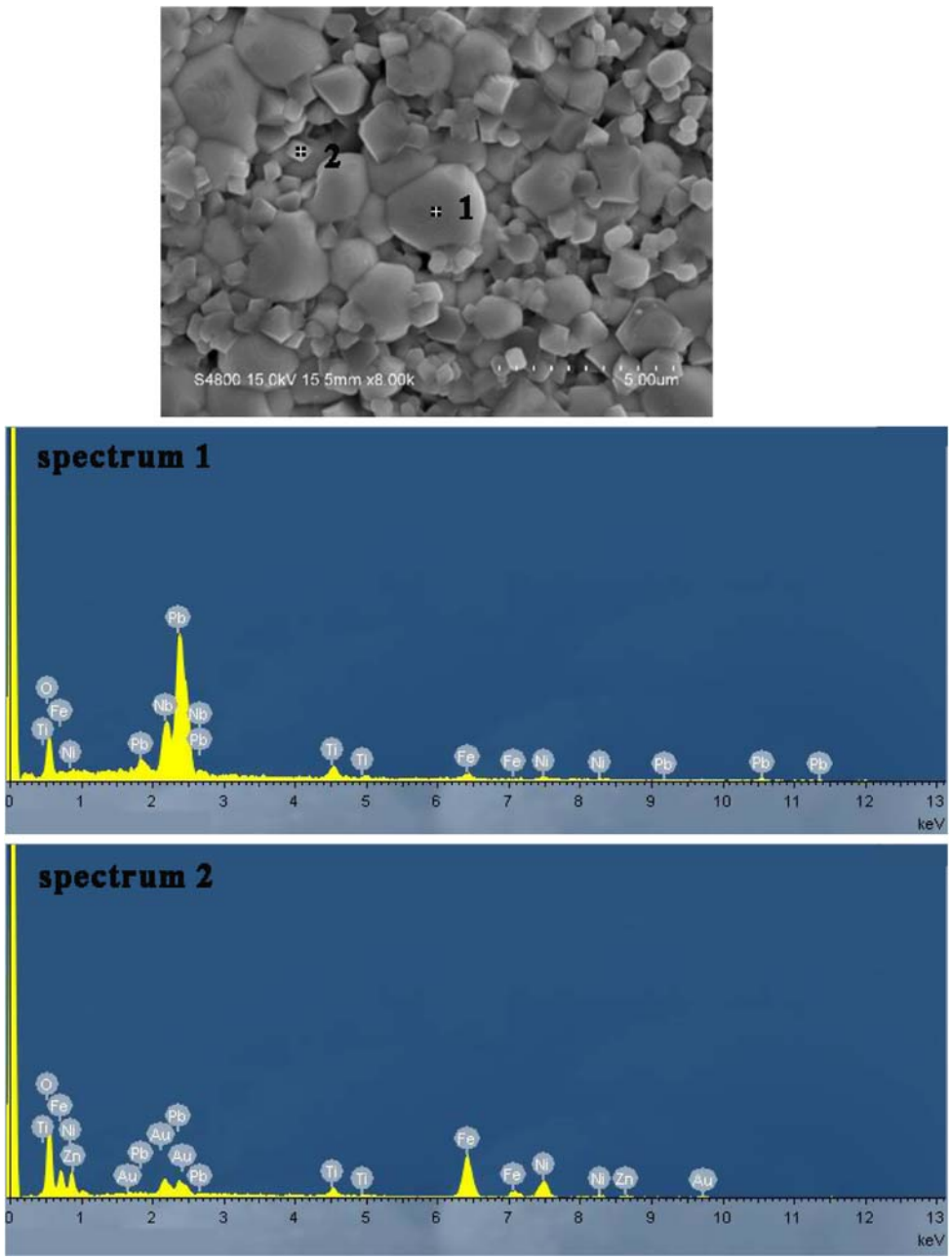

Fig. 3 EDX analysis of different grains of the 0.2NZCF/0.8PNN-PZN-PNW-PT particulate ceramic composites sintered at 950 °C for 2 h

dispersion of the composites can be attributed to the Maxwell-Wafner relaxation.

Dielectric property of the $(1-x)$NZCF/xPNN-PZN-PT composites can be improved by adding 5 mol% WO_3 in the piezoelectric phase. The improved dielectric property of the 0.1NZCF/0.9PNN-PZN-PNW-PT composites is shown in Fig. 5, where the dielectric behavior of pure PNN-PZN-PNW-PT and 0.1NZCF/0.9PNN-PZN-PT is also given for comparison. The addition of WO_3 in the piezoelectric phase not only greatly decreases dielectric loss, particularly low-frequency loss, but also greatly suppresses dielectric frequency dispersion. The decrease of T_m can be attributed to the variation of the content of piezoelectric phase and the interface effect.

Detailed dielectric property of the $(1-x)$NZCF/xPNN-PZN-PNW-PT composites ($x = 1.0$, $x = 0.9$, $x = 0.8$, $x = 0.7$, weight ratio) sintered at 950 °C for 2 h is shown in Fig. 6. At room temperature, dielectric constant of $(1-x)$NZCF/xPNN-PZN-PNW-PT decreases gradually with the increase of NZCF content accompanied by the great suppression of the dielectric frequency dispersion. Dielectric loss of $(1-x)$NZCF/xPNN-PZN-PNW-PT is also greatly decreased accordingly. The peak of dielectric loss of the composites shifts to low frequency with the increase of the

Table 1 Chemical composition of different grains of the 0.2NZCF/0.8PNN-PZN-PNW-PT particulate ceramic composites obtained by EDX analysis

Content of element	Spectrum 1		Spectrum 2	
	wt%	mol%	wt%	mol%
O	19.25	65.31	22.59	54.70
Ti	4.00	4.54	2.59	2.09
Fe	3.52	3.42	33.48	23.23
Ni	3.12	2.89	23.83	15.72
Zn	0.00	0.00	2.20	1.31
Nb	16.98	9.92	0.00	0.00
Cu	0.00	0.00	8.25	1.62
Pb	53.12	13.92	7.07	1.32

The analysis location is shown in Fig. 3

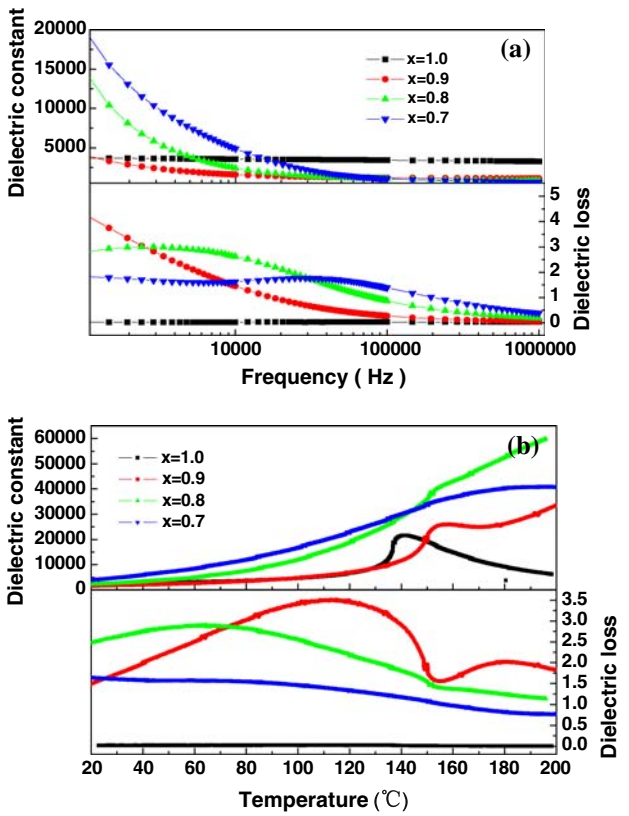

Fig. 4 Frequency and temperature dependence of dielectric constant and loss tangent of the $(1-x)$NZCF/xPNN-PZN-PT particulate ceramic composites ($x = 1.0$, $x = 0.9$, $x = 0.8$, $x = 0.7$, weight ratio) sintered at 1180 °C for 2 h. **a** Dielectric property as a function of frequency measured at room temperature. **b** Dielectric property as a function of temperature measured at 10 kHz upon heating

content of piezoelectric phase, which is considered as relating to the decrease of the amount of the accumulated space charges between the interfaces. Dielectric response peaks of the $(1-x)$NZCF/xPNN-PZN-PNW-PT composites become apparent where T_m tends to increase with the content

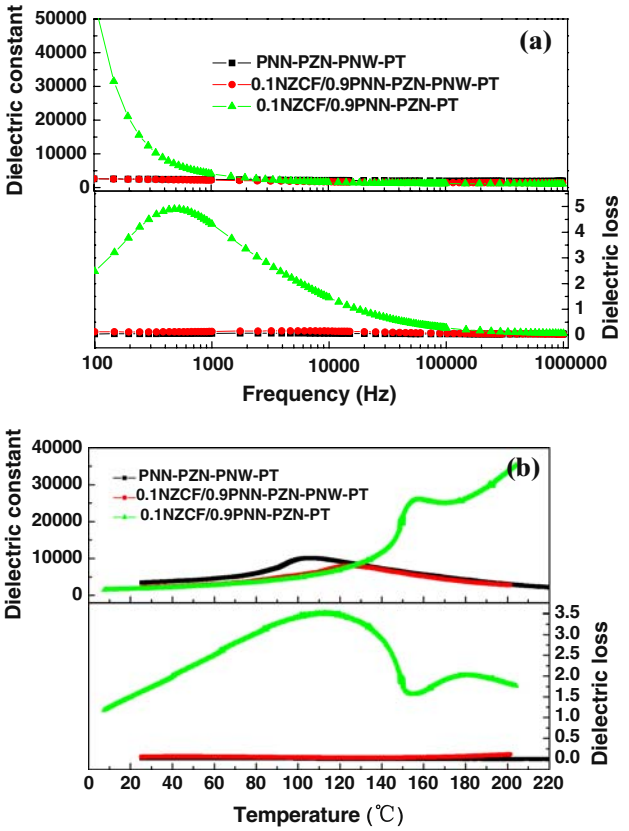

Fig. 5 Improved dielectric property of the 0.1NZCF/0.9PNN-PZN-PNW-PT particulate ceramic composites sintered at 950 °C for 2 h. **a** Dielectric property as a function of frequency measured at room temperature. **b** Dielectric property as a function of temperature measured at 10 kHz upon heating

of NZCF. Dielectric constant and loss tangent also decrease greatly as compared to those of the undoped $(1-x)$NZCF/xPNN-PZN-PT composites.

The mechanism of WO_3 doping on improving dielectric property of the magnetoelectric particulate ceramics composites is discussed in a simple way. The strong dielectric frequency dispersion and large dielectric loss of $(1-x)$NZCF/xPNN-PZN-PT can be attributed to the additional local charge compensation and the interface polarization since the piezoelectric phase and ferrite phase exhibit different dielectric permittivity and conductivity. When an electric field is applied to the composites, space charge field is induced in the ferroelectric grains near the interfaces, which contributes additional to the dielectric response. The ferrite particles reduce the local depolarization field to some extent by creating leakage paths. The diffusion of Fe^{3+} from the ferrite phase to the piezoelectric phase is another important reason, which is affected greatly by ionic radius and ionic concentration difference between the piezoelectric phase and the ferrite phase. At the same sintering conditions, ions with smaller radius and higher concentration gradient possess higher diffusion coefficient.

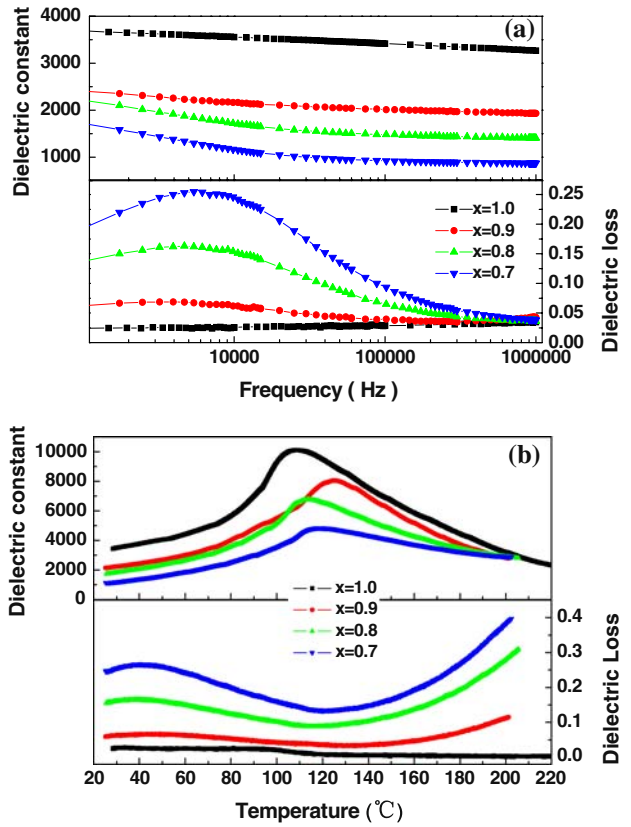

Fig. 6 Frequency and temperature dependence of dielectric constant and loss tangent of the $(1-x)$NZCF/xPNN-PZN-PNW-PT particulate ceramic composites ($x = 1.0$, $x = 0.9$, $x = 0.8$, $x = 0.7$, weight ratio) sintered at 950 °C for 2 h. **a** Dielectric property as a function of frequency measured at room temperature. **b** Dielectric property as a function of temperature measured at 10 kHz upon heating

Since the ionic radius of Fe^{3+} 0.645 Å is smaller than that of Zn^{2+} 0.740 Å, Pb^{2+} 1.19 Å, and Ni^{2+} 0.69 Å, furthermore, the concentration difference of Fe^{3+} is the largest between the piezoelectric phase and the ferrite phase, Fe^{3+} diffuses easily into the piezoelectric phase. Such consideration is confirmed by EDX analysis, which is shown in Fig. 3 and Table 1 where the piezoelectric phase contains 3.42 mol% Fe^{3+}. During sintering the diffused Fe^{3+} is partially reduced to Fe^{2+} ions, the coexistence of Fe^{3+} and Fe^{2+} cations on equivalent crystallographic sites engenders finite hopping/jump type of conduction mechanism [28], which is partially responsible for the dielectric frequency dispersion and the large value of dielectric loss, thus greatly deteriorates dielectric property of the composites. The diffusion coefficient of Fe^{3+} can be decreased by the addition of WO_3 in the piezoelectric phase, since WO_3 doping decreases sintering temperature greatly from 1180 °C to 950 °C. WO_3 can react with PbO to form liquid phase $PbWO_4$ whose melting point is around 870 °C. The appearance of liquid phase is beneficial for the dissolve, diffuse, and rearrange of particles, therefore produces dense microstructure through liquid sintering mechanism at low sintering temperature. What is more, W^{6+} tends to replace the B-site ions, which lead to the distortion of the perovskite cell lattice as shown by XRD patterns and the unbalance of charge. The lead vacancies are generated in order to compensate charge unbalance, which promotes diffusion and is beneficial for the decrease of sintering temperature. Accompanied by the decrease of sintering temperature, ions diffusion becomes slowly according to Arrhenius-type equation, $D = D_0 \exp(-E/RT)$. Where D is the diffusion coefficient, E is the activation energy of diffused specie, R is the ideal gas constant, T is the absolute temperature, and D_0 is the pre-exponential term. According to Arrhenius-type equation, the diffusion coefficient of Fe^{3+} decreases greatly due to the sharp decrease of sintering temperature induced by WO_3 doping.

Piezoelectric and ferroelectric properties of the composites

Figure 7 shows piezoelectric constant d_{33} of the $(1-x)$NZCF/xPNN-PZN-PNW-PT composites. Although the value of d_{33} of the pure PNN-PZN-PNW-PT ferroelectric is 310 pC/N, it decreases sharply and almost linearly with the addition of ferrite. When the content of ferrite increases to 30 wt%, the value of d_{33} of 0.3NZCF/0.7PNN-PZN-PNW-PT decreases to a very small value of 68 pC/N. Such decrease of piezoelectric constant is considered as correlating with the high conductivity of ferrite phase. With the increase of ferrite content, electrical poling cannot be sufficient even at high electric field due to the diffusion of low resistant ferrite into ferroelectric matrix, which deteriorates piezoelectric property of the composites.

Figure 8 shows the P–E dielectric hysteresis loops of the $(1-x)$NZCF/xPNN-PZN-PNW-PT composites. The magnetoelectric particulate ceramic composites also exhibit

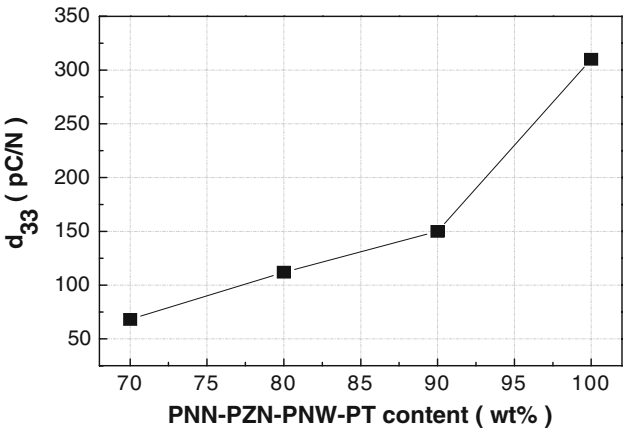

Fig. 7 Piezoelectric property of the $(1-x)$NZCF/xPNN-PZN-PNW-PT particulate ceramic composites sintered at 950 °C for 2 h as a function of the content of PNN-PZN-PNW-PT

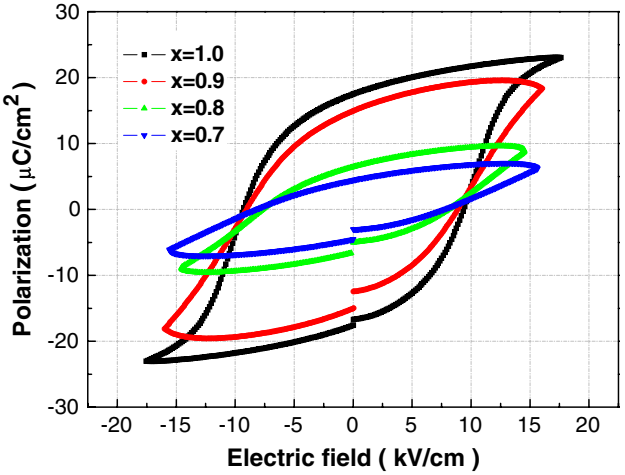

Fig. 8 P–E dielectric hysteresis loops of the (1−*x*)NZCF/*x*PNN-PZN-PNW-PT particulate ceramic composites sintered at 950 °C for 2 h

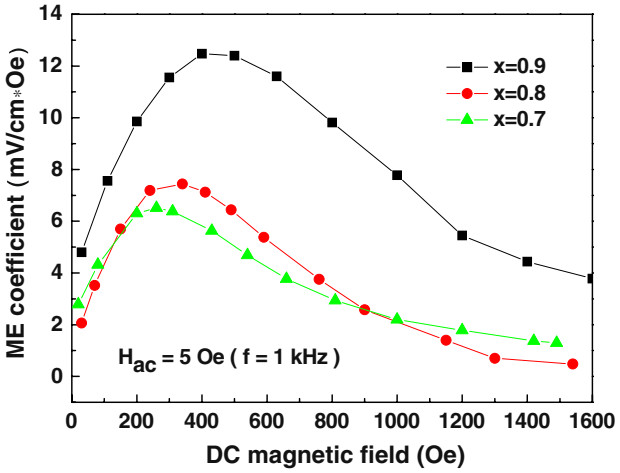

Fig. 9 Magnetoelectric voltage coefficient as a function of d.c. magnetic bias field superimposed 1 kHz a.c. magnetic field with 5 Oe amplitude at room temperature of the (1−*x*)NZCF/*x*PNN-PZN-PNW-PT particulate ceramic composites sintered at 950 °C for 2 h

typical P–E hysteresis loops. However, with the increase of ferrite content, remnant polarization (P_r) decreases greatly of the composites, while coercive filed (E_c) maintains almost invariable. P_r of the pure PNN-PZN-PNW-PT ferroelectric is about 17.5 μC/cm^2, which decreases to 15 μC/cm^2 for 0.1NZCF/0.9PNN-PZN-PNW-PT and then to a very small value of 4.5 μC/cm^2 for 0.3NZCF/0.7PNN-PZN-PNW-PT. Such character can be attributed to the semiconductivity of ferrite phase and the ion diffusion between piezoelectric and ferrite phases. The existence of leakage current also produces the open character of the hysteresis loops.

Magnetoelectric properties of the composites

The ME effect of the present system is studied as a function of the ferroelectric weight fraction. Figure 9 shows the ME voltage coefficient of the (1−*x*)NZCF/*x*PNN-PZN-PNW-PT composites as a function of d.c. magnetic bias field superimposed 1 kHz a.c. magnetic field with 5 Oe amplitude at room temperature. The ME coefficient increases with the increase of magnetic bias field and saturates at a magnetic bias field of 280–400 Oe depending on composition. For all the composites the largest ME value is obtained at a d.c. magnetic bias field less than 400 Oe, indicating that the magnetostrictive phase reaches a saturation value. The ME effect, which is considered as a product property of composites, is strongly influenced by the composition ratio of the piezoelectric phase and ferrite phase and the connectivity between the granules of the above phases. The maximum ME voltage coefficient of the composites appears at a low weight ratio of ferrite, i.e., 10 wt% ferrite phase, in which the largest ME coefficient is 13.1 mV/(cm Oe) at 1 kHz a.c. magnetic field with 5 Oe amplitude. This is due to the fact that the dielectric permittivity of the piezoelectric and ferrite phases is different and plays some important role in the ME conversion. Although the ME coefficient is not large enough, large ME effect can be obtained if the magnitude of the a.c. magnetic field increases and the frequency of the a.c. magnetic field increases to the resonant frequency of the piezoelectric phase. With the increase of ferrite content the ME voltage coefficient decreases. The decrease of ME coefficient can be attributed to the high conductivity of the ferrite phase, which deteriorates the piezoelectric property of the piezoelectric phase due to the difficulty of poling of the piezoelectric phase induced by the addition of ferrite phase.

Conclusions

A novel magnetoelectric particulate ceramic composite system composed of $Pb(Ni_{1/3}Nb_{2/3})O_3$–$Pb(Zn_{1/3}Nb_{2/3})O_3$–$Pb(Ni_{1/2}W_{1/2})O_3$–$PbTiO_3$ ferroelectric and $Ni_{0.8}Zn_{0.1}Cu_{0.1}Fe_2O_4$ ferrite were prepared by low-temperature sintering process. Dielectric property of the (1−*x*)NZCF/*x*PNN-PZN-PNW-PT particulate ceramic composites is greatly improved as compared to that of the undoped (1−*x*)NZCF/*x*PNN-PZN-PT composites. The WO_3-doped (1−*x*)NZCF/*x*PNN-PZN-PT composites can be electrically and magnetically poled to exhibit apparent ME effect. A ME voltage coefficient up to 13.1 mV/(cm Oe) is obtained at 400 Oe d.c. magnetic bias field superimposed 1 kHz a.c. magnetic field with 5 Oe amplitude for the 0.1NZCF/0.9PNN-PZN-PNW-PT composite. The addition of WO_3 in the piezoelectric phase can greatly decrease sintering temperature and dielectric loss of the composites, therefore the ME voltage coefficient increases. Such ceramic processing is

useful for the preparation of magnetoelectric particulate ceramic composites.

Acknowledgements The authors thank the International Scientific Cooperation Project of Changzhou Scientific Bureau (Grant No. CZ2008014) and the Natural Science Fundamental Research Project of Jiangsu Colleges and Universities (Grant No. 08KJB430001) for financial support.

References

1. Smolenskii GA, Chupis IE (1982) Ferroelectromagnets Sov Phys Usp 25:475
2. Suchetelene JV (1972) Philips Res Rep 27:28
3. Shin KH, Inoue M, Arai KI (2000) Smart Mater Struct 9:357
4. Ryu J, Priya S, Uchino K, Kim HE (2002) J Electroceram 8:107
5. Singh RS, Bhimasankaram T, Kumar GS (1994) Solid State Commun 91:567
6. Kornev I, Bichurin M, Rivera JP, Gentil S (2000) Phys Rev B 62:1247
7. Fuentes L, García M, Bueno D, Fuentes ME (2006) Ferroelectrics 336:81
8. Suryanarayana SV (1994) Bull Mater Sci 17(7):1259
9. Van den Boomgaard J, Terrell DR (1974) J Mater Sci 9:1705. doi:10.1007/BF00540770
10. Van den Boomgaard J, Born RAJ (1978) J Mater Sci 13:1538. doi:10.1007/BF00553210
11. Dai YR, Bao P, Zhu JS, Wan JG (2004) J Appl Phys 96(10):5687
12. Srinivasan G, DeVreugd CP, Flattery CS (2004) Appl Phys Lett 85(13):2550
13. Mazumder S, Bhattacharya GS (2004) Ceram Int 30:389
14. Mahajan RP, Patankar KK, Kothale MB (2000) Bull Mater Sci 23(4):273
15. Patankar KK, Patil SA, Sivakumar KV (2000) Mater Chem Phys 65:97
16. Dong Sh-X, Zhai J-Y, Li J-F, Viehland D, Summers E (2007) J Appl Phys 101:124102
17. Bichurin MI, Filippov DA, Petrov VM (2003) Phys Rev B 68:132408
18. Bichurin MI, Viehland D, Srinivasan G (2007) J Electroceram 19:243
19. Islam RA, Priya S (2008) J Mater Sci 43:2072. doi:10.1007/s10853-007-2442-8
20. Babu SN, Srinivas K, Suryanarayana SV, Bhimasankaram T (2008) J Phys D Appl Phys 41:165407
21. Wang Y-J, Zhao X-Y, Luo H-S (2008) J Appl Phys 103:124511
22. Nan C-W, Bichurin MI, Dong Sh-X, Viehland D, Srinivassan G (2008) J Appl Phys 103:031101
23. Liou Y-C, Chuang C-J, Shih Y-C (2005) Mater Chem Phys 93:26
24. Gao F, Qu Sh-B, Yang Z-P (2002) J Mater Sci Lett 21:15
25. Li Y-J, Chen X-M, Hou R-Z, Tang Y-H (2006) Solid State Commun 137:120
26. Lemanov VV, Sotnikov AV, Smirnova EP, Weihnacht M (2002) Phys Solid State 44:2039
27. Turik A, Radchenko G (2002) J Phys D Appl Phys 35:1188
28. Sun R-B, Tan W, Fang B-J (2009) Phys Status Solidi A 206:326